

# Journal of Nuclear Research and Applications

Research Paper

Journal homepage: <https://jonra.nstri.ir>



## An Innovative Approach for Predicting Concrete Moisture Content Based on Gamma Ray Attenuation and Artificial Neural Networks

R. Panahi<sup>1</sup>, H. Jafari<sup>1\*</sup>, M. Azizi<sup>1</sup>, M. Rahimi<sup>1</sup>, H. Kargaran<sup>2</sup>

<sup>1</sup>Department of Radiation Application, Shahid Beheshti University, Postal Code: 1983969411, Tehran, Iran.

<sup>2</sup> Faculty of Engineering, Shahed University, Postal Code: 3319118651, Tehran, Iran.

(Received: 13 July 2024, Revised: 15 October 2024, Accepted: 4 November 2024)

### ABSTRACT

Concrete is commonly used to shield gamma rays and neutrons. The effectiveness of concrete shielding for neutrons depends on the moisture content in the concrete. Moreover, the strength and durability of concrete structures are influenced by the moisture content in the concrete specimen. Therefore, determining the moisture content in concrete is crucial. The gamma ray attenuation technique is a potentially attractive non-destructive method for determining the concrete moisture content due to its high accuracy and speed. In this study, gamma attenuation in concrete shields of varying thicknesses and moisture levels was simulated using the Monte Carlo method. Two separate artificial neural networks (ANN) were trained with simulation data to accurately estimate results and decrease calculation time. The thickness of concrete is predicted in the first ANN. Then, the count in the full energy peak and thickness is applied to the second ANN to determine the concrete moisture. The trained neural network can estimate the thickness of concrete with a main relative error (MRE) of 0.42%. The findings indicate that the suggested approach can accurately determine the concrete moisture with an MRE error of 4.6% for test data.

**Keywords:** *Moisture content; Gamma-ray attenuation; Monte Carlo; Artificial neural network.*

### 1. Introductions

Highly penetrating nuclear radiation, particularly neutron and gamma rays, pose significant risks to both living organisms and the environment if not adequately attenuated. Consequently, neutron and gamma-ray shielding represent critical considerations in

radiation applications [1]. Materials exhibiting effective attenuation properties against both gamma rays and neutrons are preferred for radiation shielding purposes. Concrete, renowned for its robust capacity to attenuate both types of radiation, is commonly utilized. Its

\*Corresponding Author E-mail: [h.jafari@sbu.ac.ir](mailto:h.jafari@sbu.ac.ir)

DOI: <https://doi.org/10.24200/jonra.2024.1607.1128>.

Further distribution of this work must maintain attribution to the author(s) and the published article's title, journal citation, and DOI.

neutron shielding capabilities are augmented by its low atomic number and the inclusion of hydrogen [2,3]. Additionally, concrete is valued for its relative affordability, ease of preparation in various forms, and favorable mechanical properties. Consequently, it finds extensive use in shielding applications across nuclear power plants, accelerators, research reactors, and similar facilities [4-6]. Concrete comprises a blend of cement, small aggregates, and water. Furthermore, its chemical properties, including the presence of non-evaporating chemical water, significantly influence its effectiveness as a radiation shield [3]. The strength and longevity of concrete structures are not solely determined by their moisture content but are predominantly affected by the distribution of moisture within the concrete matrix. Hence, understanding the moisture content of concrete over time and location is essential for extracting permeability information from porous structures. Conversely, fluctuations in concrete moisture content can lead to structural defects such as cracks and corrosion [7]. Moreover, the moisture content plays a crucial role in determining the effectiveness of concrete as a shield against neutron radiation [8]. There are various methods available, both destructive and non-destructive, for assessing concrete moisture levels. One destructive method involves slicing specimens at different heights and measuring the change in mass gravimetrically for each sample [9]. On the non-destructive side, techniques such as computed tomography (CT), nuclear magnetic resonance (NMR), neutron radiography (NR), electrical methods, gamma transmission, X-ray radiography, microwave testing, and thermal

conductivity measurements are commonly employed [10,11]. Radioactive methods, known for their high accuracy and efficiency, hold promise for concrete moisture determination. Among these non-destructive approaches, gamma transmission and X-ray radiography, along with gamma and neutron radiography, depend on the attenuation of either photons as well as neutrons [7,12-16]. Each method presents its advantages and limitations. For instance, X-rays, having lower energy compared to gamma rays, may not penetrate thick samples effectively, thus posing limitations in certain applications.

Priyada [7] studied the potential of the gamma scattering technique to assess moisture content in concrete. They compared the results with those obtained from gamma transmission and traditional gravimetric methods. Their experimental setup included a collimated  $^{137}\text{Cs}$  radioactive source and a high-resolution HPGe detector. Seven concrete samples, each measuring  $5 \times 5 \times 5 \text{ cm}^3$  and with a density of  $2.4 \text{ g/cm}^3$ , were prepared, each containing different amounts of moisture. The findings showed a close agreement between the results obtained through gamma scattering and those from gravimetric and transmission methods, with an accuracy within 6%.

Klysz and colleagues [17] used direct transmitter-receiver radar waves to measure the moisture content of concrete covers. In their study, they prepared twelve concrete samples with two different compositions, varying in porosity and aggregate sizes. Each sample was saturated to different homogeneous degrees. They found that the test speed remained consistent across frequencies ranging from

300 MHz to 1.2 GHz under these conditions. Furthermore, they established a linear correlation between the volume of moisture content and the propagation velocity of the direct wave for two different partially saturated concrete mixes.

Bucurescu and colleagues [18] demonstrated the use of the gamma-ray Compton backscattering technique for determining moisture content in building materials. Their experimental setup included  $^{241}\text{Am}$  as a radiation source and a Lanthanum Bromide ( $\text{LaBr}_3$ ) detector. They concluded that measuring Compton backscattering provides a valuable, non-destructive method for assessing moisture content in porous building materials.

Machine learning techniques, such as artificial neural networks (ANN), offer innovative approaches to establishing regression relationships between variables. Xiaoli and colleagues [19] used ANN to predict soil moisture content at various depths using meteorological data as inputs, achieving results that closely align with real data. Ronghua [20] improved ANN by replacing the traditional activation function with a complex number domain and training the network based on a multi-layer perceptron structure. This modification resulted in a 9.1% improvement in prediction accuracy compared to the traditional back-propagation (BP) neural network, enhancing the theoretical basis for soil moisture prediction. Additionally, Kashif Gill [21] addressed dimensionality issues in neural networks by employing support vector machines to predict soil moisture, achieving an accuracy of 89%.

ANNs function as predictive models that anticipate the response of new sets of data. One

notable advantage is that the majority of complex computations occur during the training process. Once an ANN is trained for a specific task, operations become relatively swift, allowing for rapid identification of unknown samples in the field [22].

The objective of this study is to measure concrete moisture levels through gamma-ray attenuation. To achieve this, MCNPX, a Monte Carlo radiation transport code, has been employed to produce the the required data. However, a significant challenge arises from the extended simulation time required when using this code for gamma transmission in concrete. Therefore, an artificial neural network emerges as a viable alternative for predicting moisture levels in concrete based on gamma-ray attenuation simulation results. The neural network is trained using simulation results obtained from concrete samples with varying thicknesses and porosities through MCNPX. Parameters such as counts in the full energy peak and photo fraction are used as input variables to predict both concrete moisture content and thickness using the artificial neural network.

## 2. Materials and methods

### 2.1. Monte Carlo simulation

The simulation was conducted using the MCNPX code, a versatile Monte Carlo radiation transport tool designed to expedite computational results [23]. Developed over the past three decades at Los Alamos National Laboratory, MCNPX stands as a cutting-edge Monte Carlo code, capable of handling 36 elementary particles across all energy ranges [24]. With its advanced geometry features and utilization of continuous-energy cross-sections,

MCNPX can produce benchmark-quality results for various nuclear applications. Its robust, fully three-dimensional, combinatorial geometry allows for the modeling of complex real-world scenarios. Furthermore, the utilization of point-wise cross-sections ensures accurate reproduction of material transport properties for neutrons and photons, eliminating the need for compromises in selecting group cross-sections. The code also offers extensive customization options for problem sources, enabling detailed user-designed specifications. Additionally, the ability to perform particle flux measurements (tallies) on user-defined surfaces and volumes, coupled with statistical tests to ensure convergence criteria for each tally and prevent undersampling, enhances its utility [24,25].

A radioisotope source of  $^{137}\text{Cs}$  emitting a single gamma energy of 662 keV was positioned within a lead shield equipped with a parallel collimator to generate a focused gamma beam. Additionally, a 1-inch NaI(Tl) gamma-ray detector was placed opposite the source to capture the transmitted rays. The schematic representation of the simulated setup is illustrated in Fig. 1. In all simulations, the distances between the gamma-ray source and the concrete sample, as well as between the detector and the concrete sample, are set to 1.5 cm and 1 cm, respectively. The thickness of the concrete varies between 1 cm and 20 cm, with a fixed surface area of  $5 \times 5 \text{ cm}^2$ . The energy spectrum of photons detected by the NaI(Tl) detector was recorded using the pulse height calculation tally (F8). Furthermore, a Gaussian energy broadening card (GEB) was integrated into the simulation to replicate the peak broadening phenomenon observed in real spectra, attributed to the resolution of the detector.

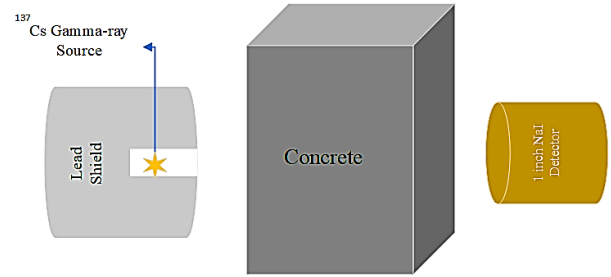


**Fig. 1.** The schematic of the simulated setup configuration to measure moisture content and thickness.

The density of concrete, which is influenced by its moisture content, is known as porosity and can be calculated using Eq. 1.

$$\phi = \frac{\rho_m - \rho_b}{\rho_m - \rho_f} \quad (1)$$

where  $\rho_m$  is the matrix density,  $\rho_b$  is the sum of the weighted components of the bulk density,  $\rho_f$  is the fluid density and  $\phi$  is the porosity [26]. In this study, Hanford-type concrete has been simulated. Its dry density is  $2.18 \text{ g/cm}^3$  as  $\rho_m$  and the density of saturated porosity is  $2.35 \text{ g/cm}^3$  (about 12% porosity) [27]. The fluid has been also considered as water with a density of  $1 \text{ g/cm}^3$ . The weight fraction of the concrete components can be determined by Eq. 2.

$$Wf_i = \frac{(100 - \phi)Wf_{di}}{100} \quad (20)$$

where  $Wf_i$  is the weight fraction of component  $i$  and  $Wf_{di}$  is the weight fraction of the same component in dry concrete. The weight fractions for all components of Hanford concrete, from zero percent moisture content (dry concrete) to saturated levels, are summarized in Table 1. Therefore, concrete with varying thicknesses and moisture contents is placed between the gamma source and the detector.

**Table 1.** Density and weight fraction used in the simulation for different percentages of moisture content in Hanford concrete.

Moisture Percent (%)	$\rho_b$	$Wf_H$	$Wf_O$	$Wf_{Na}$	$Wf_{Mg}$	$Wf_{Al}$	$Wf_{Si}$	$Wf_K$	$Wf_{Ca}$	$Wf_{Fe}$
0(dry)	2.180000	0.004000	0.482102	0.002168	0.014094	0.069387	0.277549	0.013010	0.080229	0.057461
1	2.191919	0.005071	0.486170	0.002146	0.013953	0.068693	0.274774	0.012880	0.079427	0.056886
2	2.204082	0.006142	0.490238	0.002125	0.013812	0.067999	0.271998	0.012750	0.078624	0.056312
3	2.216495	0.007213	0.494306	0.002103	0.013671	0.067305	0.269223	0.012620	0.077822	0.055737
4	2.229167	0.008284	0.498374	0.002081	0.013530	0.066612	0.266447	0.012490	0.077020	0.055163
5	2.242105	0.009355	0.502442	0.002060	0.013389	0.065918	0.263672	0.012360	0.076218	0.054588
6	2.255319	0.010426	0.506510	0.002038	0.013248	0.065224	0.260896	0.012229	0.075415	0.054013
7	2.268817	0.011497	0.510578	0.002016	0.013107	0.064530	0.258121	0.012099	0.074613	0.053439
8	2.282609	0.012568	0.514646	0.001995	0.012966	0.063836	0.255345	0.011969	0.073811	0.052864
9	2.296703	0.013639	0.518714	0.001973	0.012826	0.063142	0.252570	0.011839	0.073008	0.052290
10	2.311111	0.014710	0.522782	0.001951	0.012685	0.062448	0.249794	0.011709	0.072206	0.051715
11	2.325843	0.015781	0.526850	0.001930	0.012544	0.061754	0.247019	0.011579	0.071404	0.051140
12	2.340909	0.016852	0.530918	0.001908	0.012403	0.061061	0.244243	0.011449	0.070602	0.050566

## 2.2. Artificial neural network

Artificial neural networks (ANNs) are mathematical systems made up of basic elements called neurons that function in parallel and are inspired by the human brain [28]. ANNs have a widerange of applications in data processing, especially in radiation detection [29,30], and are particularly effective in pattern recognition across various models [31,32]. As a result, ANNs are seen as promising for predicting moisture levels in concrete. Among ANNs, the multi-layer perceptron (MLP) is the most commonly used architecture, known for its feed-forward structure consisting of input layers, hidden layers, and an output layer [33].

Before constructing an ANN model, data preprocessing involves an essential step known as feature scaling [34]. This process becomes crucial when features exhibit different value ranges, aiming to facilitate smoother processing [35]. One prevalent form of feature scaling is normalization, where features are rescaled to

fall within the range of -1 to 1 [36,37]. The performance of the MLP model is typically assessed using metrics such as mean relative error (MRE) and root mean square error (RMSE), expressed in Eq. 4 and 5, respectively [38,39].

(4)

$$MRE(\%) = 100 \times \frac{1}{N} \sum_{i=1}^N \left| \frac{T_i(MC) - Y_i(Pred)}{T_i(MC)} \right|$$

$$RMSE = \left[ \frac{\sum_{i=1}^N (T_i(MC) - Y_i(Pred))^2}{N} \right]^{0.5} \quad (5)$$

In this equation, N represents the number of data points, T(MC) denotes the desired target indicated by Monte Carlo simulation values, and Y(Pred) signifies the predicted values.

In this study, an initial network was developed to predict concrete thickness. Subsequently, moisture content was determined in a second network using both thickness and transmission gamma-rays. The dataset comprised 80 samples, with 75% used for training the network and the rest for testing

(20 samples) to predict concrete thickness. Different ANN structures were tested and optimized to obtain the best ANN configuration. The network for predicting concrete thickness uses the Tansing function, 6 neurons, and one hidden layer (Fig. 2). The specifications of the proposed ANN model for concrete thickness prediction are summarized in Table 2. The inputs for this model include the full energy peak count (FEPC) and the photo fraction (PF), representing the ratio of counts in the full energy peak to the total counts in the spectrum [40]. Various moisture levels and concrete thicknesses were employed during the neural network training phase.

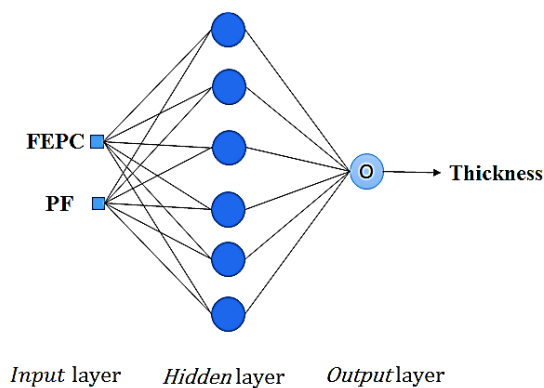


**Fig. 2.** The architecture of the proposed MLP model for concrete thickness predicting.

**Table 2.** The specifications of the proposed ANN model for concrete thickness predicting.

Neural network	MLP
Number of neurons in the input layer	2
Number of neurons in the hidden layer	6
Number of neurons in the output layer	1
Number of epochs	250
Activation function	tansig

Furthermore, various ANN structures were explored to identify the optimal configuration for determining concrete moisture. To ascertain concrete moisture content, 192 samples (approximately 80%) were allocated for

training data, while 48 samples (about 20%) were reserved for testing. Fig. 3 illustrates the proposed MLP model, featuring two hidden layers, for predicting concrete moisture. Detailed specifications of the model are provided in Table 3. The inputs for this model consist of counts in the full energy peak and concrete thickness.

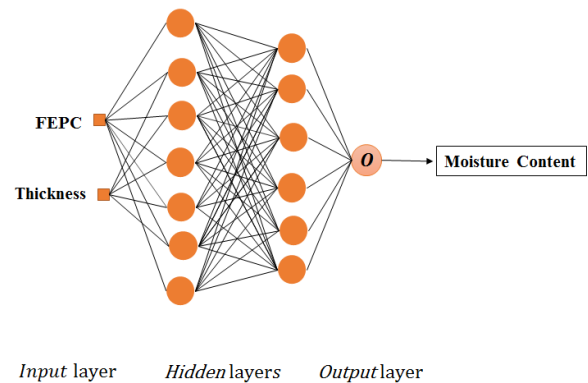


**Fig. 3.** The architecture of the proposed MLP model used for determining the concrete moisture.

**Table 3.** The specifications of the proposed ANN model for determining the concrete moisture.

Neural network	MLP
Number of neurons in the input layer	2
Number of neurons in the first hidden layer	7
Number of neurons in the second hidden layer	6
Number of neurons in the output layer	1
Number of epochs	3000
Activation function	tansig

Hence, the overall configuration of the networks used to determine concrete moisture is shown in Fig. 4.

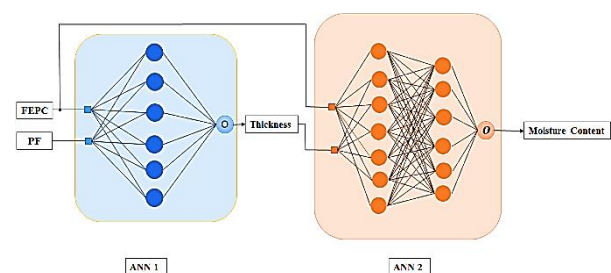


**Fig. 4.** The general pattern of the used networks for determining the concrete moisture.



### 3. Results and discussion

Gamma-ray pulse height spectra were collected for each concrete thickness and moisture content. Additionally, the FEPC was then determined by calculating the area under the full energy peak, as shown in Fig. 5, for various thicknesses and moisture contents.

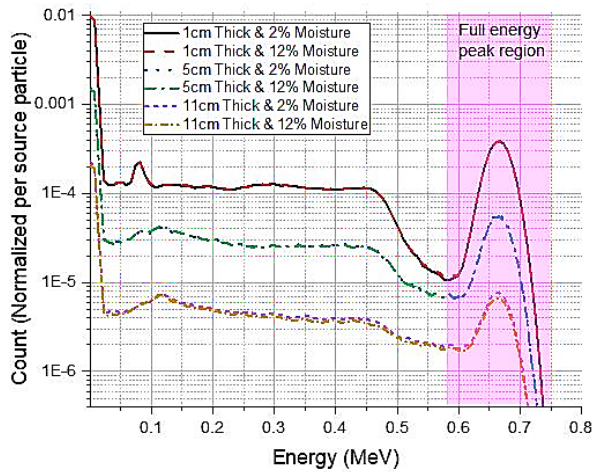


**Fig. 5.** Full energy peaks for transmitted gamma rays from concrete at several thicknesses and moisture contents.

A comparison between the simulation and predicted Artificial Neural Network results for the testing data is presented in Table 4. The standard deviation of differences was found to be 0.060 for the testing results and 0.730 for the training data.

A regression plot provides a graphical representation of the comparison between simulated and predicted results. A more accurate network tends to exhibit greater linearity, with data points closer to the  $y = x$  line. Figure 6 illustrates a regression plot for concrete thickness prediction, depicting the simulated and predicted results. It is evident that the predicted results obtained using the ANN closely align with the simulated results. The correlation coefficients are calculated to be 0.999 for both the testing and training datasets.

**Table 4.** Comparison between the MC simulated and predicted results used for network testing in concrete thickness determination.

FEPC	PF	Thickness (cm)	Predicted Thickness (cm)	Differences	FEPC	PF	Thickness (cm)	Predicted Thickness (cm)	Differences
$2.69 \times 10^{-3}$	$8.739 \times 10^{-2}$	1	0.994	0.006	$6.30 \times 10^{-5}$	$7.650 \times 10^{-2}$	11	11.125	-0.125
$1.56 \times 10^{-3}$	$8.467 \times 10^{-2}$	2	2.002	-0.002	$4.79 \times 10^{-5}$	$7.663 \times 10^{-2}$	12	12.050	-0.050
$9.70 \times 10^{-4}$	$8.237 \times 10^{-2}$	3	2.987	0.013	$3.70 \times 10^{-5}$	$7.775 \times 10^{-2}$	13	13.025	-0.025
$6.40 \times 10^{-4}$	$8.062 \times 10^{-2}$	4	4.021	-0.021	$2.81 \times 10^{-5}$	$7.788 \times 10^{-2}$	14	13.911	0.089
$4.31 \times 10^{-4}$	$7.885 \times 10^{-2}$	5	5.012	-0.012	$2.16 \times 10^{-5}$	$7.863 \times 10^{-2}$	15	14.958	0.042
$3.01 \times 10^{-4}$	$7.769 \times 10^{-2}$	6	6.008	-0.008	$1.73 \times 10^{-5}$	$7.955 \times 10^{-2}$	16	15.964	0.036
$2.16 \times 10^{-4}$	$7.773 \times 10^{-2}$	7	7.043	-0.043	$1.29 \times 10^{-5}$	$7.874 \times 10^{-2}$	17	17.080	-0.080
$1.54 \times 10^{-4}$	$7.577 \times 10^{-2}$	8	7.961	0.039	$9.81 \times 10^{-6}$	$7.676 \times 10^{-2}$	18	17.845	0.155
$1.13 \times 10^{-4}$	$7.578 \times 10^{-2}$	9	8.943	0.057	$7.93 \times 10^{-6}$	$7.900 \times 10^{-2}$	19	19.029	-0.029
$8.47 \times 10^{-5}$	$7.614 \times 10^{-2}$	10	9.987	0.013	$6.03 \times 10^{-6}$	$7.908 \times 10^{-2}$	20	19.976	0.024

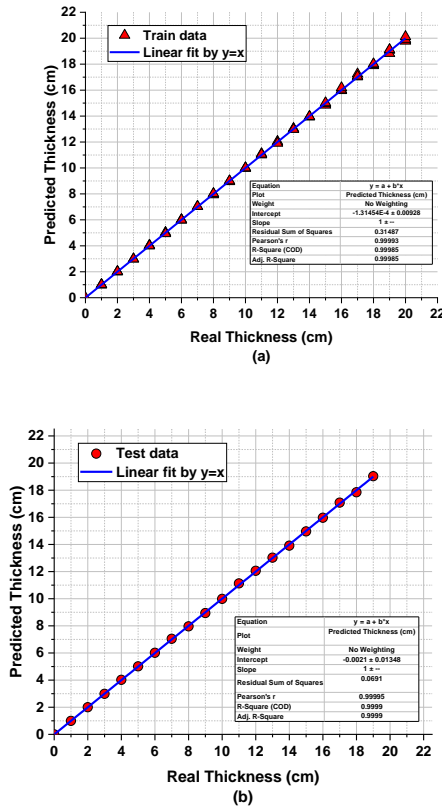


Fig. 2. The regression diagram for a) train data, b) test data in thickness prediction.

The error values for the optimal fit model of the proposed MLP model are presented in Table 5. As indicated by the table, the concrete thicknesses were determined with high precision.

Table 5. Statistical Error indices for training and testing results of concrete thickness predicting MLP model.

Error index	Train	Test
MRE (%)	0.44	0.42
RMSE	0.072	0.059

A comparison of moisture content between the Monte Carlo simulation and predicted ANN results for the testing data is presented in Table 6. The standard deviation of differences has been calculated as 0.203 for the training results and 0.285 for the testing results.

Fig. 7 illustrates a comparison between the simulated and predicted results in the proposed

MLP model for determining concrete moisture using regression plots. Based on the error values for the best fit model provided in Table 7, the moisture contents were obtained with a mean relative error (MRE) of less than 4.6%. The results of the present study can be compared with those of Ref. [7]. However, Ref. [7] utilized gamma ray transmission and scattering techniques, along with traditional methods, to estimate the moisture content in concrete samples with dimensions of  $5 \times 5 \times 5 \text{ cm}^3$ . In the present study, the maximum difference between the actual water content and the predicted value is 0.79. In contrast, Ref. [7] reports maximum differences of 7.5 and 1.3 for the transmission and scattering methods, respectively.

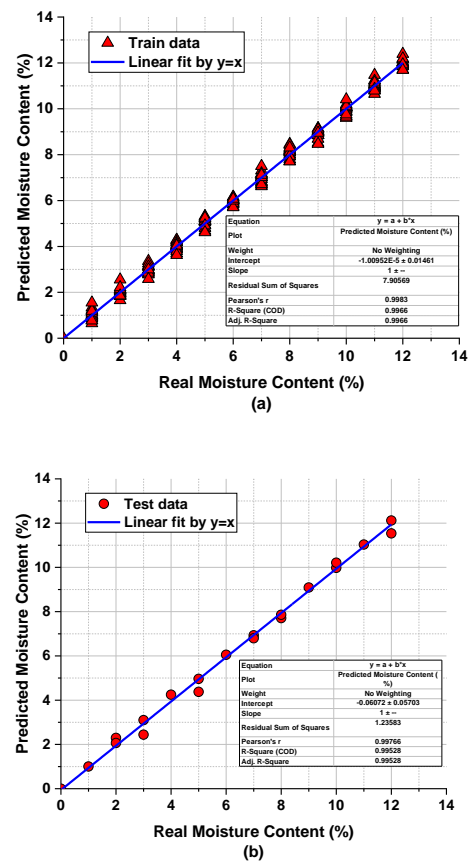


Fig. 3. Regression diagram of concrete moisture predicting ANN model for a) train data, b) test data.



**Table 6.** Comparison between the MC simulated and predicted results used for network testing in moisture content determination.

FEPC	Thickness (cm)	Moisture Content (%)	Predicted Moisture Content (%)	Differences	FEPC	Thickness (cm)	Moisture Content (%)	Predicted Moisture Content (%)	Differences
$2.69 \times 10^{-3}$	1	2	2.294	-0.294	$6.55 \times 10^{-5}$	11	2	1.940	0.060
$2.68 \times 10^{-3}$	1	7	6.930	0.070	$6.20 \times 10^{-5}$	11	7	7.128	-0.128
$2.66 \times 10^{-3}$	1	12	11.536	0.464	$5.85 \times 10^{-5}$	11	12	11.553	0.447
$1.56 \times 10^{-3}$	2	5	4.959	0.041	$4.79 \times 10^{-5}$	12	5	4.711	0.289
$1.54 \times 10^{-3}$	2	10	9.978	0.022	$4.41 \times 10^{-5}$	12	10	10.466	-0.466
$9.78 \times 10^{-4}$	3	3	3.098	-0.098	$3.76 \times 10^{-5}$	13	3	2.947	0.053
$9.65 \times 10^{-4}$	3	8	7.705	0.295	$3.51 \times 10^{-5}$	13	8	8.119	-0.119
$6.47 \times 10^{-4}$	4	1	1.000	0.000	$2.97 \times 10^{-5}$	14	1	0.873	0.127
$6.36 \times 10^{-4}$	4	6	6.050	-0.050	$2.76 \times 10^{-5}$	14	6	6.591	-0.591
$6.23 \times 10^{-4}$	4	11	11.033	-0.033	$2.57 \times 10^{-5}$	14	11	10.999	0.001
$4.35 \times 10^{-4}$	5	4	4.247	-0.247	$2.21 \times 10^{-5}$	15	4	4.105	-0.105
$4.24 \times 10^{-4}$	5	9	9.089	-0.089	$2.04 \times 10^{-5}$	15	9	9.123	-0.123
$3.06 \times 10^{-4}$	6	2	2.066	-0.066	$1.78 \times 10^{-5}$	16	2	2.306	-0.306
$2.98 \times 10^{-4}$	6	7	6.795	0.205	$1.63 \times 10^{-5}$	16	7	7.400	-0.400
$2.89 \times 10^{-4}$	6	12	12.116	-0.116	$1.51 \times 10^{-5}$	16	12	11.439	0.561
$2.15 \times 10^{-4}$	7	5	4.374	0.626	$1.32 \times 10^{-5}$	17	5	4.869	0.131
$2.06 \times 10^{-4}$	7	10	10.213	-0.213	$1.18 \times 10^{-5}$	17	10	10.138	-0.138
$1.57 \times 10^{-4}$	8	3	2.439	0.561	$1.03 \times 10^{-5}$	18	3	3.098	-0.098
$1.51 \times 10^{-4}$	8	8	7.856	0.144	$9.28 \times 10^{-6}$	18	8	8.008	-0.008
$1.19 \times 10^{-4}$	9	1	0.997	0.003	$8.43 \times 10^{-6}$	19	1	1.279	-0.279
$1.13 \times 10^{-4}$	9	6	6.238	-0.238	$7.54 \times 10^{-6}$	19	6	5.786	0.214
$1.06 \times 10^{-4}$	9	11	11.056	-0.056	$6.83 \times 10^{-6}$	19	11	10.584	0.416
$8.47 \times 10^{-5}$	10	4	3.837	0.163	$6.19 \times 10^{-6}$	20	4	3.209	0.791
$8.08 \times 10^{-5}$	10	9	8.947	0.053	$5.55 \times 10^{-6}$	20	9	9.038	-0.038

**Table 7.** Statistical Error indices for training and testing results moisture content corresponding to the proposed MLP model.

Error index	Train	Test
MRE (%)	4.10	4.60
RMSE	0.202	0.283

#### 4. Conclusion

This study introduces a new method for predicting concrete moisture levels using an appropriate ANN model in conjunction with the gamma-ray attenuation method. The research involved simulating concrete samples with varying thicknesses and porosities using the

Monte Carlo MCNPX code. The gamma transmission pulse height spectrum through the samples was recorded by a NaI detector. Two distinct multi-layer perceptron ANNs were used to estimate concrete thickness and moisture content based on the full energy peak count and photo fraction extracted from the spectrum. The findings show that the trained ANN models can predict concrete thickness and moisture content with MREs of less than 0.42% and 4.6%, respectively. This indicates the feasibility of the proposed ANN model as an accurate and reliable tool in combination with the gamma-

ray attenuation technique for determining concrete moisture content.

### Conflict of interest

The authors declare no potential conflict of interest regarding the publication of this work.

### References

- [1] Chilton AB, Shultis JK, Faw RE. [Principles of radiation shielding](#). 1984.
- [2] Julphunthong P, Joyklad P, editors. Investigation of gamma ray shielding and compressive strength of concrete containing barite and ferrophosphorous. [Key Engineering Materials](#); 2018: Trans Tech Publ.
- [3] Kaplan M. Concrete radiation shielding: nuclear physics, concrete properties, design and construction: [Longman Publishing Group](#); 1989.
- [4] Schaeffer NM. Reactor shielding for nuclear engineers. [Radiation Research Associates, Inc.](#), Fort Worth, Tex.(USA), 1973.
- [5] Jaeger RG. Engineering Compendium on Radiation Shielding: Volume I: Shielding Fundamentals and Methods: [Springer Science & Business Media](#); 2013.
- [6] Tschirf E. Concrete as a shielding material against X-rays, gamma and neutron. [Zement-und-Beton](#). 1976;21(5):240-4.
- [7] Priyada P, Ramar R. Determining the water content in concrete by gamma scattering method. [Annals of Nuclear Energy](#). 2014;63:565-70.
- [8] Hilsdorf H. A method to estimate the water content of concrete shields. [Nuclear Engineering and Design](#). 1967;6(3):251-63.
- [9] Janz M. Methods of measuring the moisture diffusivity at high moisture levels: [Lund University](#); 1997.
- [10] Wormald R, Britch A. Methods of measuring moisture content applicable to building materials. [Building science](#). 1969;3(3):135-45.
- [11] Roels S, Carmeliet J, Hens H, Adan O, Brocken H, Cerny R, et al. A comparison of different techniques to quantify moisture content profiles in porous building materials. [Journal of Thermal Envelope and Building Science](#). 2004;27(4):261-76.
- [12] Roels S, Carmeliet J. Analysis of moisture flow in porous materials using microfocus X-ray radiography. [International Journal of Heat and Mass Transfer](#). 2006;49(25-26):4762-72.
- [13] Reijonen H, Pihlajavaara S. On the determination by neutron radiography of the thickness of the carbonated layer of concrete based upon changes in water content. [Cement and concrete research](#). 1972;2(5):607-15.
- [14] Zhang P, Wittmann FH, Zhao T-j, Lehmann EH, Vontobel P. Neutron radiography, a powerful method to determine time-dependent moisture distributions in concrete. [Nuclear Engineering and Design](#). 2011;241(12):4758-66.
- [15] Kanematsu M, Maruyama I, Noguchi T, Ikura H, Tsuchiya N. Quantification of water penetration into concrete through cracks by neutron radiography. [Nuclear Instruments and Methods in Physics Research Section A: Accelerators, Spectrometers, Detectors and Associated Equipment](#). 2009;605(1-2):154-8.
- [16] Nielsen AF. Gamma-ray-attenuation used for measuring the moisture content and homogeneity of porous concrete. [Building Science](#). 1972;7(4):257-63.
- [17] Klysz G, Balayssac J-P. Determination of volumetric water content of concrete using ground-penetrating radar. [Cement and concrete research](#). 2007;37(8):1164-71.
- [18] Bucurescu D, Bucurescu I. Non-destructive measurement of moisture in building materials by compton scattering of gamma rays. [Romanian Reports in Physics](#). 2011;63(1):61-75.
- [19] Hou X, Feng Y, Wu G, He Y, Chang D. Application research on artificial neural network dynamic prediction model of soil moisture. [Water Saving Irrigation](#). 2016;7:70-2.
- [20] Cai Y, Zheng W, Zhang X, Zhangzhong L, Xue X. Research on soil moisture prediction model based on deep learning. [PloS one](#). 2019;14(4):e0214508.
- [21] Gill MK, Asefa T, Kembrowski MW, McKee M. Soil moisture prediction using support vector machines 1. [JAWRA Journal of the American Water Resources Association](#). 2006;42(4):1033-46.
- [22] Keller PE, Kouzes RT, editors. Gamma spectral analysis via neural networks. [Proceedings of 1994 IEEE Nuclear Science Symposium-NSS'94](#); 1994: IEEE.
- [23] Ringuest JL. Multiobjective optimization: behavioral and computational considerations: [Springer Science & Business Media](#); 2012.
- [24] Pelowitz D. User's manual, version of MCNPX2. 6.0, 672 [LANL](#), LA-CP-07-1473. 2008.
- [25] Kargaran H, Jafari H, Minuchehr A. A novel approach based on improved combinatorial geometry (ICG) model for photon transport in Monte Carlo codes. [Progress in Nuclear Energy](#). 2021;131:103565.
- [26] Foldiak G. [Industrial application of radioisotopes](#). 1986.

- [27] Gesh C, Pagh R, Rucker R, Williams R. Radiation portal monitor project. Compendium of material composition data for radiation transport modeling. PNNL-15870, Rev. 1. [Pacific Northwest National Laboratory](#). 2011.
- [28] Ido AS, Bonyadi M, Etaati G, Shahriari M. Unfolding the neutron spectrum of a NE213 scintillator using artificial neural networks. [Applied Radiation and isotopes](#). 2009;67(10):1912-8.
- [29] Liu G, Aspinall M, Ma X, Joyce M. An investigation of the digital discrimination of neutrons and  $\gamma$  rays with organic scintillation detectors using an artificial neural network. [Nuclear Instruments and Methods in Physics Research Section A: Accelerators, Spectrometers, Detectors and Associated Equipment](#). 2009;607(3):620-8.
- [30] Yildiz N, Akkoyun S. Neural network consistent empirical physical formula construction for neutron-gamma discrimination in gamma ray tracking. [Annals of Nuclear Energy](#). 2013;51:10-7.
- [31] Khorsandi M, Feghhi S, Salehizadeh A, Roshani G. Developing a gamma ray fluid densitometer in petroleum products monitoring applications using Artificial Neural Network. [Radiation measurements](#). 2013;59:183-7.
- [32] Salgado WL, Dam RSdF, Teixeira TP, Conti C, Salgado C. Application of artificial intelligence in scale thickness prediction on offshore petroleum using a gamma-ray densitometer. [Radiation Physics and Chemistry](#). 2020;168:108549.
- [33] Hanus R, Zych M, Jaszczur M, editors. Computational Intelligence Approach for Liquid-Gas Flow Regime Classification Based on Frequency Domain Analysis of Signals from Scintillation Detectors. [International Work-Conference on Artificial Neural Networks](#); 2019: Springer.
- [34] Raju VG, Lakshmi KP, Jain VM, Kalidindi A, Padma V, editors. Study the influence of normalization/transformation process on the accuracy of supervised classification. [2020 Third International Conference on Smart Systems and Inventive Technology \(ICSSIT\)](#); 2020: IEEE.
- [35] Ozsahin DU, Mustapha MT, Mubarak AS, Ameen ZS, Uzun B, editors. Impact of feature scaling on machine learning models for the diagnosis of diabetes. [2022 International Conference on Artificial Intelligence in Everything \(AIE\)](#); 2022: IEEE.
- [36] Elfaki EA, Ahmed AH. Prediction of electrical output power of combined cycle power plant using regression ANN model. [Journal of Power and Energy Engineering](#). 2018;6(12):17.
- [37] Yen M-H, Liu D-W, Hsin Y-C, Lin C-E, Chen C-C. Application of the deep learning for the prediction of rainfall in Southern Taiwan. [Scientific reports](#). 2019;9(1):1-9.
- [38] Taylor JG. [Neural networks and their applications](#). 1996.
- [39] Azar AT. Fast neural network learning algorithms for medical applications. [Neural Computing and Applications](#). 2013;23(3):1019-34.
- [40] Knoll GF. [Radiation detection and measurement](#): John Wiley & Sons; 2010.

**How to cite this article**

R. Panahi, H. Jafari, M. Azizi, M. Rahimi, H. Kargaran, *An Innovative Approach for Predicting Concrete Moisture Content Based on Gamma Ray Attenuation and Artificial Neural Networks*, Journal of Nuclear Research and Applications (JONRA), Volume 4 Number 4 Autumn (2024) 34-44.  
 URL: [https://jonra.nstri.ir/article\\_1691.html](https://jonra.nstri.ir/article_1691.html), DOI: <https://doi.org/10.24200/jonra.2024.1607.1128>.



This work is licensed under the Creative Commons Attribution 4.0 International License.  
 To view a copy of this license, visit <http://creativecommons.org/licenses/by/4.0>.